JOURNAL OF COMPUTATIONAL PHYSICS 34, 202–210 (1980)

Fourier Expansion Solution of the Korteweg–de Vries Equation

KANJI ABE AND OSAMU INOUE

Institute of Space and Aeronautical Science, University of Tokyo, 4-6-1 Komaba, Meguro-ku, Tokyo, Japan 153

Received May 16, 1978; revised March 22, 1979

The Korteweg–de Vries equation is numerically solved by using the Fourier expansion method, the finite-difference methods, and other methods. By applying each method to a common initial-value problem, the accuracies of computations are compared with each other. The Fourier expansion method is found to be the most accurate and effective method. The details of the recurrence of an initial state, discussed by N. J. Zabusky and M. D. Kruskal, are examined.

1. INTRODUCTION

The Korteweg–de Vries equation has been found to describe various kinds of phenomena such as acoustic waves in an anharmonic crystal, waves in bubble–liquid mixtures, magnetohydrodynamic waves in warm plamas, and ion acoustic waves. Several methods of solving this equation numerically have been proposed. Some of them are based on the finite-difference methods [1, 2, 3], where we approximate all of the differentials by appropriate finite differences and reduce the partial differential equation to a set of algebraic equations.

A numerical procedure competitive with the finite difference method is the Fourier expansion method [4, 5]. In this method, the unknown function is expanded in terms of the Fourier series, and the original partial differential equation is reduced to a set of ordinary differential equations for the Fourier coefficients. The hybrid methods, where the Fourier expansion is partially employed, have also been proposed [6, 7, 8].

This paper is concerned with the Fourier expansion method compared with the other methods. Zabusky and Kruskal [1] solved the K–dV equation using a finite-difference method, and showed the existence of solitons which propagated with their own velocities, exerting essentially no influence on each other. They also discussed the recurrence of an initial state and guessed that the K–dV equation led to the recurrence. All of the methods noted above are applied to this problem, and are compared with each other for accuracy of the numerical computations.

0021-9991/80/020202–09$02.00/0

2. Fourier Expansion Solution

Zabusky and Kruskal solved the K–dV equation

$$\frac{\partial u}{\partial t} + u\frac{\partial u}{\partial x} + \delta^2 \frac{\partial^3 u}{\partial x^3} = 0, \tag{1}$$

with $\delta = 0.022$ and the initial periodic condition

$$u(t = 0, x) = \cos(\pi x), \qquad 0 \leqslant x \leqslant 2. \tag{2}$$

The Fourier expansion corresponding to this is

$$u(t, x) = \sum_{k=-\infty}^{\infty} a_k(t) \exp(i\pi k x), \tag{3}$$

with the initial condition

$$a_k(0) = \delta_{k,\pm 1}/2, \tag{4}$$

where $\delta_{k,m}$ is the Kronecker delta. Substituting Eq. (3) into Eq. (1), we obtain

$$\begin{aligned} \frac{da_k}{dt} &= -i\pi \sum_{m=-\infty}^{\infty} m a_{k-m} a_m + i\pi^3 \delta^2 k^3 a_k \\ &= -\frac{1}{2} i\pi k \sum_{m=-\infty}^{\infty} a_{k-m} a_m + i\pi^3 \delta^2 k^3 a_k . \end{aligned} \tag{5}$$

Equations (4) and (5) lead to $a_0(t) = 0$ for all t.

In order to make truncation, we introduce the maximal wavenumber $k_{\max}$ defined by

$$a_k(t) = 0 \qquad (|\, k \,| > k_{\max}). \tag{6}$$

From the relation $a_{-k} = a_k^*$, which is obtained from the reality condition on u, it is sufficient to determine a_k $(1 \leqslant k \leqslant k_{\max})$ from Eq. (5). The time integrations of Eq. (5) are made by using the Runge–Kutta–Gill method. If we neglect the nonlinear term in Eq. (5), we obtain $a_k(t) \propto \exp(i\pi^3 \delta^2 k^3 t)$. From this we guess the temporal interval Δt by $\pi^3 \delta^2 k_{\max}^3 \, \Delta t \lesssim 1$.

The K–dV equation has the conservation laws

$$\begin{aligned} C_1 &= \left| \int_0^2 u \, dx \right| = 0, \qquad C_2 = \left| \int_0^2 u^2 \, dx - 1 \right| = 0, \\ C_3 &= \left| \frac{1}{\pi^2 \delta^2} \int_0^2 \left[\frac{1}{3} u^3 - \delta^2 \left(\frac{\partial u}{\partial x} \right)^2 \right] dx + 1 \right| = 0. \end{aligned} \tag{7}$$

If we substitute Eqs. (3) and (6) into the laws, the first law is easily shown to be automatically satisfied and the other laws become

$$C_2 = \left| 4 \sum_{k=1}^{k_{\max}} a_k a_k^* - 1 \right|,$$

$$C_3 = \left| \frac{2}{3} \frac{1}{\pi^2 \delta^2} \sum_{k=1}^{k_{\max}} \sum_{m=1}^{k_{\max}} (a_k a_m a_{k+m}^* + a_k^* a_m^* a_{k+m} + a_k^* a_m a_{k-m} + a_k a_m^* a_{k-m}^*) \right.$$

$$\left. - 4 \sum_{k=1}^{k_{\max}} k^2 a_k a_k^* + 1 \right|. \tag{8}$$

Almost all of the computations are made by using numbers of 8 figures (single precision) or, when more accurate results are required, by using numbers of 16 figures (double precision).

3. Results of the Fourier Expansion Method

If we neglect the dispersive term in the K–dV equation (1), the nonlinear term makes the derivative $\partial u/\partial x$ infinite at $t = 1/\pi$, the breakdown time. Let us write time t in the form of πt. Figure 1 shows the spectra obtained from the numerical computations using numbers of 16 figures, and setting $k_{\max} = 70$ and $\pi \Delta t = 8 \times 10^{-4}$. The spectrum of high harmonics is roughly steady for $\pi t \gtrsim 3$. This fact ensures the convergence of the present solution, that is to say, the error arising from the truncation (6) does not increase with the lapse of time. The waveforms recovered by using Eqs. (3) and (6) are shown in Fig. 2. Figure 3 shows the space–time trajectories of soliton peaks. The results shown in Figs. 2 and 3 are in good agreement with those

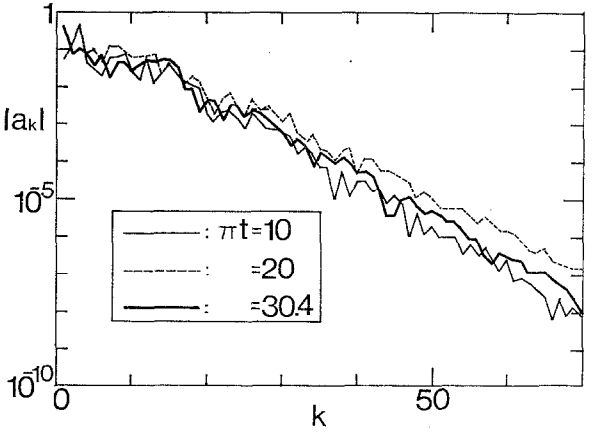

Fig. 1. Temporal development of spectrum; $k_{\max} = 70$, $\pi \Delta t = 8 \times 10^{-4}$, and 16 figures.

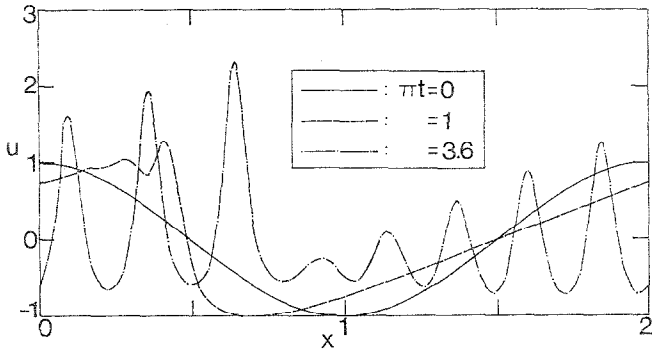

FIG. 2. Temporal development of waveform; $k_{\max} = 70$, $\pi\Delta t = 8 \times 10^{-4}$, and 16 figures.

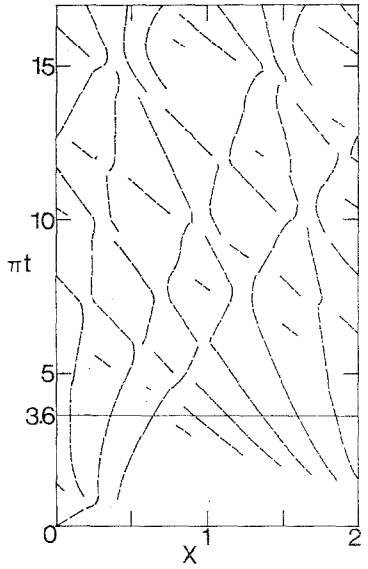

FIG. 3. Soliton-peak trajectories corresponding to Fig. 2.

of Zabusky and Kruskal. Figures 4 and 5 give the waveforms and the trajectories of solitons at the subsequent stage. The time $\pi t = 30.4$ in the figures is the recurrence time introduced by Zabusky and Kruskal. The result corresponding to Figs. 4 and 5 was not given in their paper. They guessed that at the recurrence time, all the solitons overlapped at a common spatial point and the concentration of the solitons almost reconstructed the initial monochromatic wave. We see from Figs. 4 and 5 that at $\pi t = 30.4$ all the solitons tend to focus at a common spatial point, but none of the solitons loses its identity during collisions of solitons. As shown in Fig. 1, the spectrum at $\pi t = 30.4$ is far from $|a_k| = \delta_{k1}/2$, which indicates the reconstruction of the monochromatic wave.

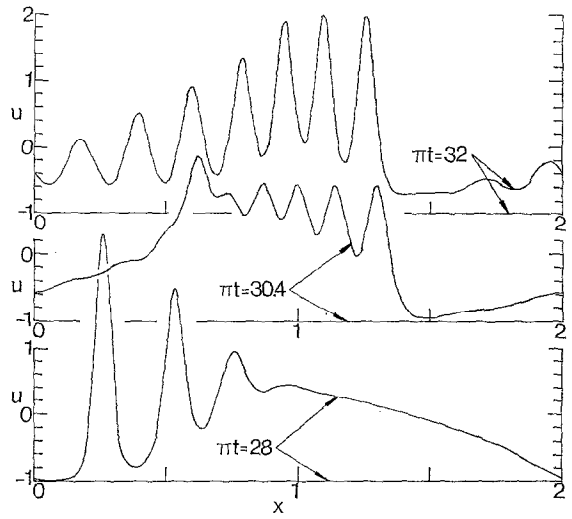

FIG. 4. Waveforms at the subsequent stage; $k_{\max} = 70$, $\pi\Delta t = 8 \times 10^{-4}$, and 16 figures.

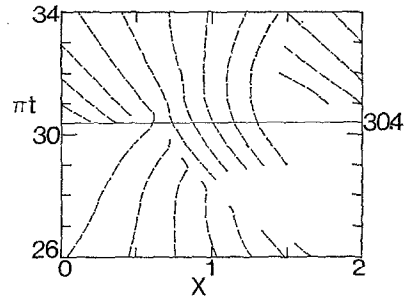

FIG. 5. Soliton-peak trajectories corresponding to Fig. 4.

In the computations noted above, the conservation laws are

$$C_2 < 2 \times 10^{-12} \quad \text{and} \quad C_3 < 5 \times 10^{-11} \quad \text{for} \quad 0 \leqslant \pi t \leqslant 34,$$

where C_2 and C_3 have been given by Eqs. (8). In order to examine the truncation errors arising from approximation (6), we made the computations changing the maximal wavenumber $k_{\max}$. In the computations, numbers of eight figures were used. Figure 6 shows how the waveform converges to the correct waveform with increasing $k_{\max}$, where we have regarded $u(t, x; k_{\max} = 70, \pi\,\Delta t = 8 \times 10^{-4}$, 16 figures) as the correct waveform $u_{\text{correct}}(t, x)$. The analytic solution [9] may give the correct waveform. We, however, do not employ the analytic solution, because the procedure for obtaining

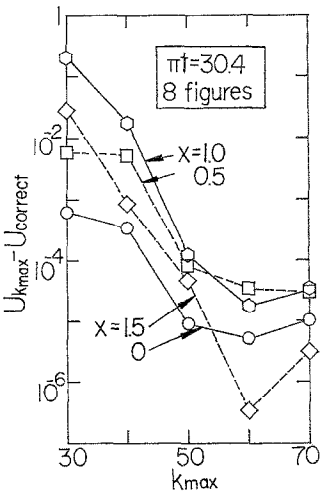

FIG. 6. Convergence of the waveform to the correct form with increasing $k_{\max}$. $u_{k\max}$ is calculated by using numbers of 8 figures. $u_{\text{correct}}(t, x) = u(t, x; k_{\max} = 70, \pi\Delta t = 8 \times 10^{-4}$, 16 figures).

the values of u from the solution is rather complicated. Figure 6 shows that the truncation errors become slight as $k_{\max}$ increases. By changing the temporal interval $\pi\,\Delta t$, the errors by the Runge–Kutta–Gill method for the integrations of Eq. (5) are examined. Figure 7 shows how the waveform approaches the correct waveform with decreasing $\pi\,\Delta t$. The integrations of Eq. (5) using $\pi\,\Delta t > 10^{-2.4}$ led to unphysical solutions, where the values of $a_k(t)$ oscillated and diverged with increasing time t. Figures 6 and 7 show that the integration of Eq. (5) using $k_{\max} = 50$, $\pi\,\Delta t = 4 \times 10^{-3} \simeq 10^{-2.4}$, and numbers of eight figures gives a sufficiently accurate solution.

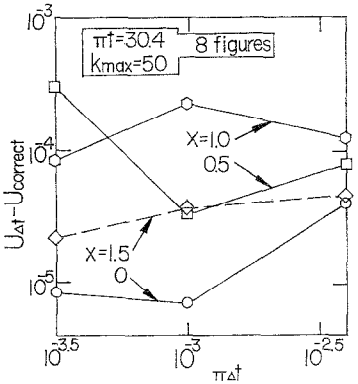

FIG. 7. Convergence of the waveform to the correct form with decreasing $\pi\Delta t$. $u_{\Delta t}$ is calculated by using $k_{\max} = 50$ and numbers of 8 figures. u_{correct} is the same as that in Fig. 6.

4. Finite-Difference Methods and Other Methods

The schemes compared with the Fourier expansion methods are

I. Zabusky–Kruskal scheme [1]:

$$u_j^{n+1} = u_j^{n-1} - \frac{\Delta t}{\Delta x}\frac{u_{j+1}^n + u_j^n + u_{j-1}^n}{3}(u_{j+1}^n - u_{j-1}^n) - \frac{\delta^2 \Delta t}{\Delta x^3}(u_{j+2}^n - 2u_{j+1}^n + 2u_{j-1}^n - u_{j-2}^n) \qquad (j = 1 \sim J), \tag{9}$$

where $u_j^n = u(t = n\,\Delta t, x = (j-1)\,\Delta x)$ and $(J-1)\,\Delta x = 2$.

II. Greig–Morris scheme [2]:

$$u_j^{n+1} = u_j^n - \frac{1}{2}\frac{\Delta t}{\Delta x}(f_{j+1}^n - f_{j-1}^n) - \frac{1}{2}\frac{\delta^2 \Delta t}{\Delta x^3}(u_{j+2}^n - 2u_{j+1}^n + 2u_{j-1}^n - u_{j-2}^n), \quad \text{for } j+n \text{ even},$$
$$u_j^{n+1} = u_j^n - \frac{1}{2}\frac{\Delta t}{\Delta x}(f_{j+1}^{n+1} - f_{j-1}^{n+1}) - \frac{1}{2}\frac{\delta^2 \Delta t}{\Delta x^3}(u_{j+2}^{n+1} - 2u_{j+1}^{n+1} + 2u_{j-1}^{n+1} - u_{j-2}^{n+1}), \quad \text{for } j+n \text{ odd}, \tag{10}$$

where $j = 1 \sim J$ and $f = u^2/2$. If we set J even and use the cyclic boundary condition, the implicit scheme (10) handles easily.

III. Gazdag scheme [6]: Reference [6] is so short that the authors could not give in detail the procedures used to execute the scheme. This method may consist of the following two steps. We compute an intermediate solution by

$$\tilde{u}(t + \Delta t, x) = u(t, x) + \frac{\partial u}{\partial t}\Delta t + \frac{1}{2}\frac{\partial^2 u}{\partial t^2}\Delta t^2 + \cdots \tag{11}$$

where

$$\frac{\partial u}{\partial t} = -u\frac{\partial u}{\partial x}, \qquad \frac{\partial^2 u}{\partial t^2} = \frac{\partial}{\partial t}\left(-u\frac{\partial u}{\partial x}\right) = 2u\left(\frac{\partial u}{\partial x}\right)^2 + u^2\frac{\partial^2 u}{\partial x^2}, \cdots. \tag{12}$$

Next we solve the linear equation

$$\frac{\partial u}{\partial t} = -\delta^2\frac{\partial^3 u}{\partial x^3},$$

which has the analytical solution

$$u(t + \Delta t, x) = \mathrm{Re}\left\{\sum_{k=1}^{\infty}\left[\int_0^2 u(t, x')\exp(-i\pi k x')\,dx'\right]\exp(i\pi^3\delta^2 k^3\,\Delta t + i\pi k x)\right\}, \tag{13}$$

where $\mathrm{Re}(f)$ means the real part of f. We put $u(t, x') = \tilde{u}(t + \Delta t, x')$.

In expansion (11) we neglect the temporal derivatives of fourth order or higher. The spatial derivatives in Eq. (12) are approximated by

$$\left.\frac{\partial u}{\partial x}\right|_j^n = \frac{u_{j+1}^n - u_{j-1}^n}{2\Delta x}, \qquad \left.\frac{\partial^2 u}{\partial x^2}\right|_j^n = \frac{u_{j+1}^n - 2u_j^n + u_{j-1}^n}{\Delta x^2},$$

$$\left.\frac{\partial^3 u}{\partial x^3}\right|_j^n = \frac{u_{j+2}^n - 2u_{j+1}^n + 2u_{j-1}^n - u_{j-2}^n}{2\Delta x^3}, \ldots \qquad (j = 1 \sim J),$$

where $(J-1)\,\Delta x = 2$. If in Eq. (13) we evaluate the value of $u(t, x')$ only on the discrete points $j = 1 \sim J$, and make the appropriate truncation of high harmonics, the FFT (Fast Fourier Transform) technique is applicable twice. We evaluate the right-hand side of Eq. (13) using the FFT technique. The high harmonics with $k > k_{\max}$ are neglected, because the inclusion of high harmonics leads to unphysical divergences in computer. We made computations changing the values of J and $k_{\max}$ within a limitation $J > k_{\max}$, and found that if we set $J = 2^9 + 1 = 513$, the case $k_{\max} = 32$ gave the best results.

5. Comparison

We made computations using the Zabusky–Kruskal, Greig–Morris, and Gazdag schemes for $10^{-3} \geqslant \pi\,\Delta t \geqslant 10^{-5}$ and $2/200 \geqslant \Delta x \geqslant 2/800$. Table I gives the results where $\pi\,\Delta t = 10^{-4}$ and $\Delta x = 2/400 \sim 2/512$. The values of C_2 and C_3 in the schemes of Zabusky and Kruskal, Greig and Morris, and Gazdag have been defined in Eqs. (7), while those of the Fourier expansion method have been defined in Eqs. (8). The derivative $\partial u/\partial x$ required to determine C_3 in the schemes of Zabusky and Kruskal, Greig and Morris, and Gazdag is calculated from

$$\partial u/\partial x\,|_j^n = (u_{j+1}^n - u_{j-1}^n)/(2\Delta x).$$

The values of C_2 and C_3 in the table show that the Fourier expansion method using numbers of 16 figures gives the most accurate solution. Let us measure the error of each scheme by

$$E = \left(\Delta x \sum_{j=1}^{J-1} |\, u_j^n - u_{j,\text{correct}}^n\,|^2\right)^{1/2},$$

where $n\pi\,\Delta t = 1$, $(J-1)\,\Delta x = 2$, and $u_{j,\text{correct}}^n = u$ $(\pi t = 1,\ x = (j-1)\,\Delta x$; $k_{\max} = 70$, $\pi\,\Delta t = 8 \times 10^{-4}$, 16 figures). The values of E are included in Table I.

The computations using various sets of $(\Delta t, \Delta x)$ showed that there was little correlation between C_2 and $(\Delta t, \Delta x)$. The Zabusky–Kruskal scheme (9) with $\pi\,\Delta t = 10^{-5}$ and $\Delta x = 2/800$ gives, among the schemes other than the Fourier expansion method, the most accurate waveforms, which are in good agreement with those in Figs. 2 and 3. The Zabusky–Kruskal scheme, however, is numerically unstable and does not give

TABLE I

Comparison between the Fourier Expansion Method and Other Methods

	Zabusky–Kruskal	Greig–Morris	Gazdag	Fourier expansion method	
$\pi\Delta t$	10^{-4}	10^{-4}	10^{-4}	4×10^{-3}	8×10^{-4}
Δx	2/400	2/401	2/512		
k_{max}				50	70
			No. of figures		
	8	8	8	8	16
$C_2(\pi t = 1)$	3.2×10^{-8}	4.2×10^{-5}	1.0×10^{-3}	1.0×10^{-6}	6.6×10^{-15}
$C_3(\pi t = 1)$	2.1×10^{-2}	2.0×10^{-2}	3.3×10^{-2}	1.6×10^{-6}	1.1×10^{-13}
E	9.3×10^{-4}	9.5×10^{-4}	8.9×10^{-4}	2.4×10^{-6}	0

the solution for $\pi t > 17$. The Greig–Morris scheme and the Gazdag scheme are numerically stable, but the accuracies of computations become so much worse with increasing time that we have no confidence that the numerical solutions at large times are correct.

In addition to the schemes noted above, we examined two more schemes. One is an implicit finite-difference scheme proposed by Goda [3]. The other is the Taylor–Fourier expansion method proposed by Canosa and Gazdag [8]. Detailed procedures for putting the schemes into execution are not given in the respective papers. The Goda scheme may not be appropriate to the present problem, where the waveform shows a rather complicated variation with the lapse of time. The Canosa–Gazdag scheme may consume too much computation time to obtain the solutions with sufficient accuracy.

REFERENCES

1. N. J. ZABUSKY AND M. D. KRUSKAL, *Phys. Rev. Lett.* **15** (1965), 240.
2. I. S. GREIG AND J. LL. MORRIS, *J. Comput. Phys.* **20** (1976), 64.
3. K. GODA, *J. Phys. Soc. Japan* **39** (1975), 229.
4. H. SCHAMEL AND K. ELSÄSSER, *J. Comput. Phys.* **22** (1976), 501.
5. S. WATANABE, M. OHISHI, AND H. TANACA, *J. Phys. Soc. Japan* **42** (1977), 1382.
6. J. GAZDAG, *J. Comput. Phys.* **13** (1973), 100.
7. F. TAPPERT, *Lectures in Appl. Math.* **15** (1974), 215.
8. J. CANOSA AND J. GAZDAG, *J. Comput. Phys.* **23** (1977), 393.
9. H. P. MCKEAN AND P. VAN MOERBEKE, *Invent. Math.* **30** (1975), 217.